Pulse lead/lag timing detection for adaptive feedback and control based on optical spike-timing-dependent plasticity

Mable P. Fok,[1],* Yue Tian,[1] David Rosenbluth,[2] and Paul R. Prucnal[1]

[1]*Lightwave Communication Research Laboratory, Department of Electrical Engineering, Princeton University, Princeton, New Jersey 08544, USA*

[2]*Lockheed Martin Advanced Technologies Laboratory, Cherry Hill, New Jersey 08002, USA*
Corresponding author: mfok@princeton.edu

Biological neurons perform information processing using a model called pulse processing, which is both computationally efficient and scalable, adopting the best features of both analog and digital computing. Implementing pulse processing with photonics can result in bandwidths that are billions of times faster than biological neurons and substantially faster than electronics. Neurons have the ability to learn and adapt their processing based on experience through a change in the strength of synaptic connections in response to spiking activity. This mechanism is called spike-timing-dependent plasticity (STDP). Functionally, STDP constitutes a mechanism in which strengths of connections between neurons are based on the timing and order between presynaptic spikes and postsynaptic spikes, essentially forming a pulse lead/lag timing detector that is useful in feedback control and adaptation. Here we report for the first time the demonstration of optical STDP that is useful in pulse lead/lag timing detection and apply it to automatic gain control of a photonic pulse processor.   © 2013 Optical Society of America
   OCIS codes: 070.4340, 320.7085.

Neuromorphic engineering [1,2] has a wide range of applications, such as adaptive control, learning, perception, motion control, sensory processing, and autonomous robots. Realization of biological neurons solely with photonics harnesses the high speed and wide bandwidth of optics, opening a host of new applications for ultrafast decision making and adaptability. Photonic neurons capable of processing signals at terahertz rates and a simple photonic-neuron circuit mimicking the tail-flip escape response in crayfish have recently been demonstrated [3–6]. Like those of its physiological counterpart, the functions performed by the photonic neuron are determined by the configuration of a set of parameters including the weights and delays of interconnections, the temporal integration time, and the spiking threshold.

Learning in neurons is accomplished with a set of synaptic weights that are adjusted based upon the activity of the system in response to its inputs. The standard model for learning in systems of spiking neurons is called spike-timing-dependent plasticity (STDP) [7–10]. STDP is a learning mechanism where the generated neuronal responses are based on the input and output timing, order, and sequence. Figure 1(a) illustrates the schematic of unsupervised learning in neurons. Although the feedback path introduces latency to the weight adjustment, it does not affect the capacity or speed of the photonic neuron itself. In STDP, the relative timing of pre- and postsynaptic spikes determines the changes to the strength of the synapse as follows:

• Pre-post firing: a presynaptic spike precedes a postsynaptic spike and is presumed to have contributed to causing the postsynaptic spike. Therefore, the synaptic connection is "rewarded" or strengthened, causing a "potentiation."

• Post-pre firing: a presynaptic spike follows a postsynaptic spike and could not have contributed to causing

the post-synaptic spike. Therefore, the synaptic connection is "punished" or weakened, causing a "depression."

Figure 1(b) illustrates the STDP behavior of a biological neuron, where the shaded region is the potentiation window while the unshaded region is the depression window. In other words, STDP is performing pulse lead/lag timing detection, in which a different output intensity is returned from STDP in response to different input timing, order, and sequence. The STDP output can be used for adaptive feedback and control of a system. STDP rules have been previously been applied to coincidence detection [11], sequence learning [12–14], path learning in navigation [15,16], and directional selectivity in visual response [16,17]. The STDP approach to learning has not only received attention in application-based contexts but also as a general expressive learning rule for cognitive computing. It is demonstrably equivalent to near-optimal information-theoretic algorithms [18–20], such as relevant mutual information maximization, information bottleneck optimization, and independent component analysis.

The operation of optical STDP is analogous to its physiological counterpart in that the strength of the optical interconnection is increased in response to pre-post firing while it is decreased for post-pre firing. Optical STDP operates on picosecond time scales, which
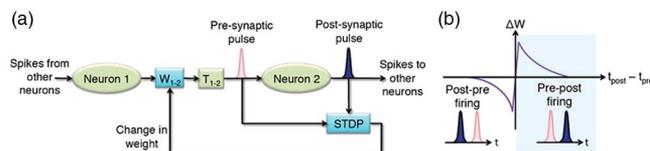

Fig. 1.   (Color online) (a) Unsupervised learning with STDP. (b) STDP characteristic. $t_{post}-t_{pre}$: time interval between the post- and presynaptic spikes. ΔW: resultant change in synaptic strength.

are achieved by exploiting fast physical mechanisms in photonic devices, such as absorption saturation in electro-absorption modulators (EAMs) [21] and gain depletion in semiconductor optical amplifiers (SOAs) [22].

Optical STDP is illustrated in Fig. 2(a). It takes both the post- and presynaptic spikes and splits them unequally such that a larger portion of the postsynaptic spike goes to the SOA (Kamelian SOA-NL-L1-C-FA) and a larger portion of the presynaptic spike goes to the EAM (CIP 10G-PS-EAM-1550). The postsynaptic spike induces gain depletion in the SOA, and the resulting gain is experienced by the presynaptic spike. The presynaptic spike induces absorption saturation in the EAM, and the resulting absorption is experienced by the postsynaptic spike. Optical bandpass filters are used to extract the pre- and postsynaptic spikes from the SOA and EAM outputs, respectively. They are then detected using a photodetector. Figures 2(b) and 2(c) illustrate the mechanism for optical STDP. When a strong postsynaptic spike enters the SOA, it immediately depletes the SOA gain. Thus, if a presynaptic spike enters the SOA shortly after the postsynaptic spike [Fig. 2(b)], it experiences the minimum gain (the weakest output power). The gain gradually recovers over time due to the presence of the SOA driving current, and the output power of the presynaptic spike gradually increases as the time interval between the post- and presynaptic spikes increases, forming the depression window (region I). If a presynaptic spike enters the SOA before the postsynaptic spike [Fig. 2(c)], it does not experience any gain depletion, and the output power remains the same (region II). In the EAM, the absorption is large due to the reverse bias, and no absorption saturation is experienced by the postsynaptic spike when it enters the EAM before the strong presynaptic spike, resulting in a weak output power (region III). When the postsynaptic spike enters the EAM shortly after the presynaptic spike, a strong absorption saturation is experienced by the postsynaptic spike, resulting in a strong output power. The EAM absorption
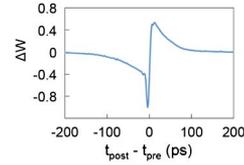
Fig. 3. (Color online) Experimentally measured optical STDP characteristic.

builds up gradually over time due to the reverse bias, resulting in a gradual decrease in output power of the postsynaptic spike, forming the potentiation window (region IV). By linearly combining the effects in SOA and EAM, an STDP characteristic results [Fig. 2(d)].

In our experiment, the input powers of the presynaptic and postsynaptic spikes are both 10 dBm with ~5 ps pulse width. Figure 3 shows the experimentally measured STDP responses using the proposed optical STDP configuration, which resembles the physiological STDP characteristic. As with biological STDP, optical STDP allows independent control of the width and height of the potentiation and depression windows to implement different functions. The potentiation-window width decreases as the EAM bias increases [Fig. 4(a)], resulting from the stronger electro-absorption effect under a stronger bias, while the depression-window width decreases as the SOA current increases [Fig. 4(b)] due to the increase in carrier density in the SOA under a stronger injection current. The ratio between the potentiation and depression window heights changes as the pre- and postsynaptic spikes' splitting ratio varies [Fig. 4(c)]. As shown in Fig. 4(d), the height of the potentiation window is independently adjustable by changing the spikes' power launch to the EAM.

Using the proposed optical STDP, we experimentally demonstrate automatic gain control of a photonic pulse processor in which a "teacher" determines the way the photonic pulse processor should spike in response to its input (1551.72 nm). The teacher (1550.12 nm) first presents the processor with the correct response (presynaptic spike) [Fig. 5(a)], and then STDP compares the processor output (1553.33 nm) (postsynaptic spike)
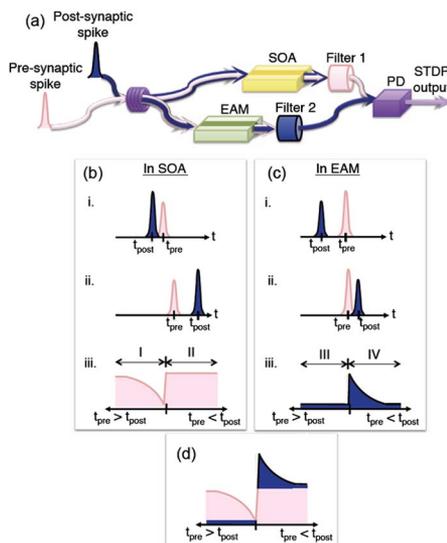
Fig. 2. (Color online) (a) Optical implementation of STDP. (b) Formation of depression window. (c) Formation of potentiation window. (d) Linearly combining (b) and (c) results in STDP characteristic.
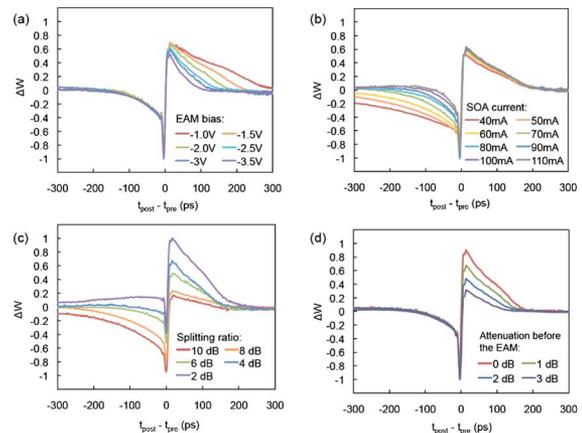
Fig. 4. (Color online) (a) Reconfigurable STDP characteristic. (b) Different SOA driving current. (c) Different pre- and postsynaptic spikes splitting ratio. (d) Different input power to the EAM.
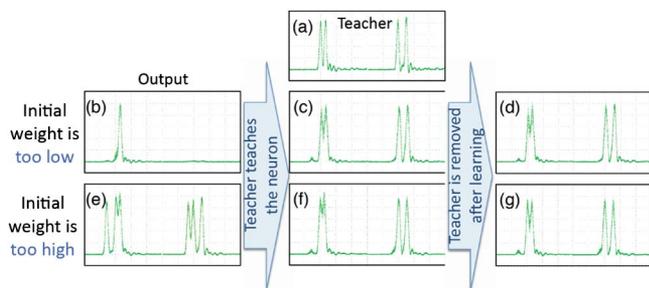
Fig. 5. (Color online) Experimental results of automatic gain control in pulse-processing device based on optical STDP. (a) Correct response presented by the teacher; (b)–(d) initial weight is too low, and the optical STDP adjusts its gain automatically; (e)–(g) initial weight is too high, and the optical STDP adjust its gain automatically.

with the teacher input. If the photonic pulse processor is not spiking in the way the teacher wants, STDP makes changes to the interconnection strength by sending the amount of weight change determined by the optical STDP to the weighting device. In this experiment, an EOM is used as a weighting device to govern the interconnection strength.

Figures 5(b) and 5(e) show two examples of the pulse-processor output when it is not spiking correctly. In Fig. 5(b) the interconnection strength is too weak, while in Fig. 5(e) the interconnection strength is too strong. With the optical STDP enabled, the pulse processor automatically adjusts the strength of the interconnection based on the result from STDP. Figures 5(c) and 5(f) show the processor output after it has learned from the teacher, where it is now spiking in way the teacher expects after adjusting itself based on the result from STDP. After the learning phase, the teacher is removed, and the processor still spikes in the way that the teacher expects [Figs. 5(d) and 5(g)], indicating that the photonic pulse processor has learned from the teacher.

In summary, we proposed and successfully demonstrated for the first time, to our knowledge, optical STDP and automatic gain control for photonic pulse processing. This is not only an important milestone enabling photonic neurons to perform learning but also provides an automatic way for adaptive feedback and control in various systems. STDP modifies synaptic strengths based on the correlation between the pre- and postsynaptic activities. Our optical STDP utilized the inherent properties of two optical devices, an EAM and a SOA, that

naturally mimic biological STDP characteristics. Just like its biological counterpart, variable potentiation and depression windows are achieved in optical STDP, satisfying the requirements of diverse types of synapses and applications.

References

1. J. J. Hopfield and D. W. Tank, Science **233**, 625 (1986).
2. M. Mahowald and R. A. Douglas, Nature **354**, 515 (1991).
3. D. Rosenbluth, K. Kravtsov, M. P. Fok, and P. R. Prucnal, Opt. Express **17**, 22767 (2009).
4. M. P. Fok, D. Rosenbluth, K. Kravtsov, and P. R. Prucnal, IEEE Signal Process. Mag. **27**, 160 (2010).
5. K. Kravtsov, M. P. Fok, D. Rosenbluth, and P. R. Prucnal, Opt. Express **19**, 2133 (2011).
6. M. P. Fok, H. Deming, M. Nahmias, N. Rafidi, D. Rosenbluth, A. Tait, Y. Tian, and P. R. Prucnal, Opt. Lett. **36**, 19 (2011).
7. S. Song, K. D. Miller, and L. F. Abbott, Nat. Neurosci. **3**, 919 (2000).
8. R. C. Froemke and Y. Dan, Nature **416**, 433 (2002).
9. N. Caporale and Y. Dan, Annu. Rev. Neurosci. **31**, 25 (2008).
10. G. Bi and M. Poo, Annu. Rev. Neurosci. **24**, 139 (2001).
11. W. Gerstner, R. Kempter, J. L. V. Hemmen, and H. Wagner, Nature **383**, 76 (1996).
12. A. A. Minai and W. B. Levy, in *INNS World Congress of Neural Networks II* (Erlbaum, 1993), pp. 505–508.
13. L. F. Abbott and K. I. Blum, Cereb. Cortex **6**, 406 (1996).
14. P. D. Roberts, J. Comput. Neurosci. **7**, 235 (1999).
15. K. I. Blum and L. F. Abbott, Neural Comput. **8**, 85 (1996).
16. M. R. Mehta, M. C. Quirk, and M. Wilson, Neuron **25**, 707 (2000).
17. R. Rao and T. J. Sejnowski, in *Advances in Neural Information Processing Systems 12* (MIT, 2000), pp. 164–170.
18. G. Chechik, Neurocomputation **15**, 1481 (2003).
19. L. Buesing and W. Maass, in *Advances in Neural Information Processing Systems 20* (MIT, 2007), pp. 193–200.
20. C. Savin, P. Joshi, and J. Triesch, PLoS Comput. Biol. **6**, e1000757 (2010).
21. M. Suzuki, H. Tanaka, and S. Akiba, Electron. Lett. **25**, 88 (1989).
22. M. Koga, N. Tokura, and K. Nawata, Appl. Opt. **27**, 3964 (1988).